

Impact of the New Radiation Package McRad in the ECMWF Integrated Forecast System

Jean-Jacques Morcrette 
European Centre for Medium-Range Weather Forecasts
Shinfield Park, Reading RG2 9AX, United Kingdom

The Monte-Carlo Independent Column Approximation (McICA) was recently introduced by Barker et al. (2003) and Pincus et al. (2003) as a flexible way to ensure an unbiased, if noisy, description of the radiative fields over appropriate time and space scales in a large-scale model of the atmosphere.

McICA is introduced here as part of a new radiation transfer package (McRad) for the ECMWF forecast model and tested in both low-resolution ($T_159 L91$) seasonal simulations and higher resolution ($T_319 L91$) ten-day forecasts. The package includes an McICA version of both the RRTM_LW and RRTM_SW radiation schemes, a revision of the cloud optical properties, and a new surface albedo derived from MODIS data. The impact is assessed through comparisons of model fields with corresponding observations and of objective scores against those obtained with the operational radiation configuration.

In long simulations, McRad has a marked effect in reducing some systematic errors in the position of tropical convection, due to change in the overall distribution of diabatic heating over the vertical, inducing a geographical redistribution of the centres of convection.

At high resolution, with respect to forecasts carried out with the standard radiation schemes, McRad has a small (generally positive) on objective scores of the geopotential and a larger impact on temperatures, with a warming of the lower troposphere and a cooling of the upper troposphere and lower stratosphere.

Finally, the flexibility of McICA approach in dealing with cloud overlap and cloud inhomogeneity is illustrated in an additional series of seasonal simulations with the cloud generator and McRad handling either a generalized overlapping inhomogeneous clouds or the previously assumed maximum-random overlapping plane-parallel clouds.

	RRTM_LW	RRTM_SW
Solution of RT Equation	Two-stream method	Two-stream method
Number of spectral intervals	16 (140 g-points)	14 (112 g-points)
Absorbers	$H_2O, CO_2, O_3, CH_4, N_2O, CFC11, CFC12, aerosols$	$H_2O, CO_2, O_3, CH_4, N_2O, CFC11, CFC12, aerosols$
Spectroscopic database	HITRAN, 1996	HITRAN, 1996
Absorption coefficients	From LBLRTM line-by-line model	From LBLRTM line-by-line model
Cloud handling	True cloud fraction	True cloud fraction
Cloud optical properties		
Method	16-band spectral emissivity from τ, g, ω	14-band τ, g, ω
Data:	Ebert & Curry, 1992	Ebert & Curry, 1992
Ice clouds	Fu et al., 1998	Fu, 1996
Water clouds	Smith & Shi, 1992	Fouquart, 1987
Lindner & Li, 2000	Lindner & Li, 2000	Slingo, 1989
Cloud overlap assumption set up in cloud generator	Maximum-random or generalized	Maximum-random or generalized
Reference	Mlawer et al., 1997	Mlawer and Clough, 1997

Table 1 Characteristics of the longwave and shortwave radiation schemes in McRad.

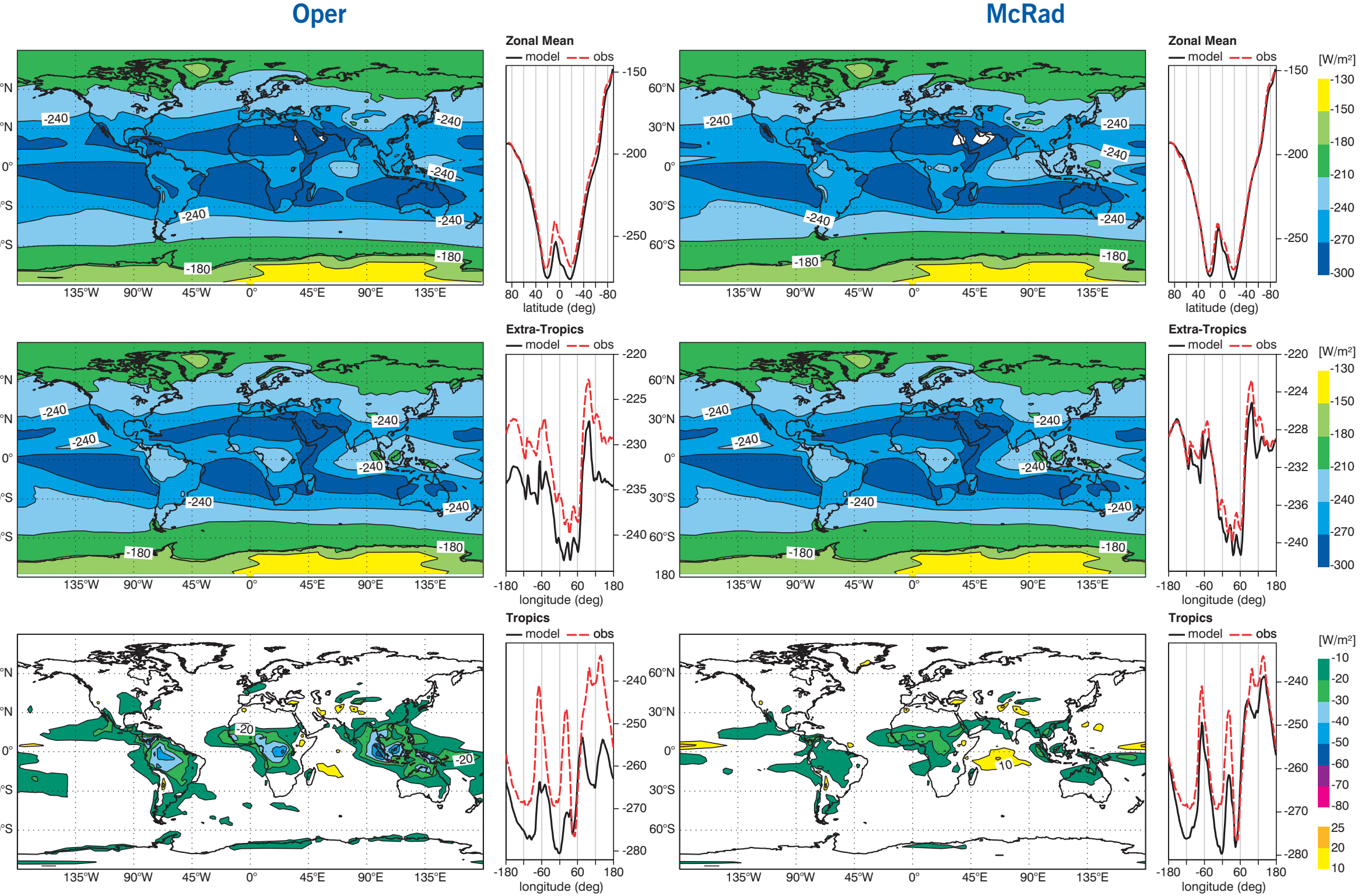


Figure 1 The outgoing longwave radiation at the top of the atmosphere ($W m^{-2}$). Top figures are the ECMWF model simulations (left: operational, right: McRad), middle ones are the CERES observations, bottom ones are the differences between simulations and observations.

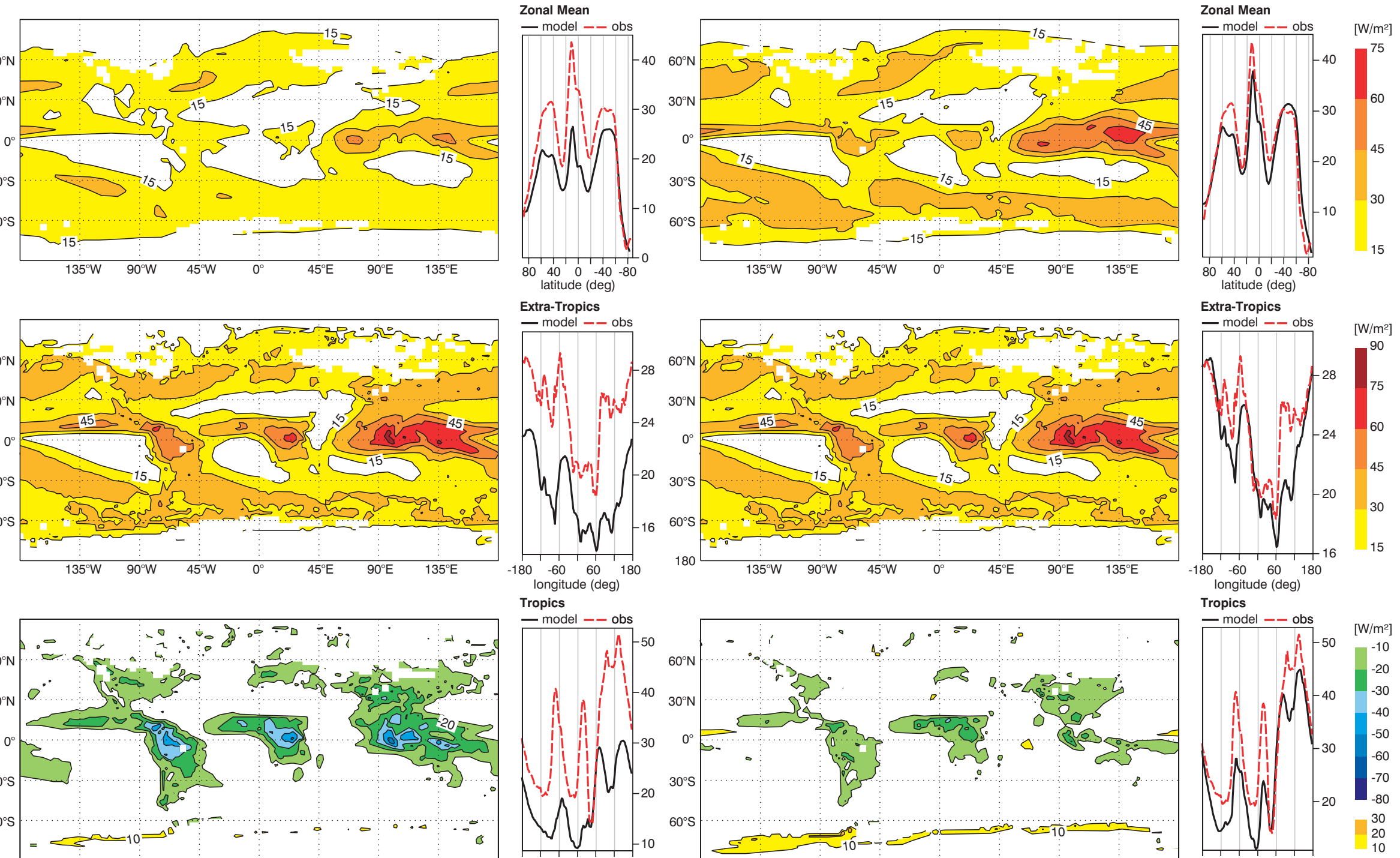


Figure 2 The absorbed shortwave radiation in the atmosphere ($W m^{-2}$). Top figures are the ECMWF model simulations (left: operational, right: McRad radiation), middle ones are the CERES observations, bottom ones are the differences between simulations and observations.

	Annual	DJF	JJA
OLR	-239	-236	-242
Oper	-8.1 (12.7)	-6.1 (15.0)	-5.1 (12.8)
McRad	-3.2 (7.9)	-1.1 (10.1)	-0.6 (10.5)
ASW	244	251	238
Oper	-10.0 (17.5)	-15.6 (23.9)	-9.2 (19.7)
McRad	-5.8 (14.2)	-11.4 (20.5)	-5.3 (18.6)
LWCF	27.3	26.8	26.1
Oper	-9.6 (13.6)	-10.4 (16.5)	-8.3 (14.1)
McRad	-4.0 (7.9)	-4.8 (10.3)	-3.0 (9.7)
SWCF	-48.7	-52.8	-45.1
Oper	-5.2 (15.4)	-4.1 (18.6)	-6.3 (18.2)
McRad	-0.2 (12.9)	0.5 (17.0)	-1.3 (17.3)
TCWV	29.0	27.7	29.3
Oper1	-2.10 (3.65)	-2.27 (4.29)	-1.73 (3.69)
McRad	-1.67 (3.13)	-1.80 (3.63)	-1.25 (3.32)
TCC	62.2	62.9	61.4
Oper	-6.0 (10.3)	-5.7 (12.3)	-5.4 (11.8)
McRad	-5.3 (9.5)	-4.9 (11.2)	-4.7 (11.4)
TCLW	82.2	80.4	84.3
Oper	1.67 (22.1)	3.13 (33.4)	-1.11 (30.6)
McRad	0.86 (22.4)	2.05 (32.8)	-1.21 (30.8)
TP gpcp	2.61	2.58	2.63
Oper	0.45 (1.39)	0.42 (1.88)	0.43 (1.75)
McRad	0.40 (1.21)	0.37 (1.60)	0.41 (1.72)
TP ssmi	3.80	3.57	3.66
Oper	0.67 (2.45)	0.57 (3.56)	0.44 (3.90)
McRad	0.50 (2.23)	0.38 (3.32)	0.35 (3.81)
SSR ocn	155.2	163.7	143.7
Oper	8.4	15.1	0.3
McRad	15.6	21.9	7.4
STR ocn	-51.8	-52.5	-50.4
Oper	0.6	1.0	1.3
McRad	-0.1	0.3	0.6
SSH ocn	-11.0	-13.7	-9.0
Oper	-4.7	-3.0	-5.9
McRad	-3.5	-2.0	-4.9
SLH ocn	-96.5	-100.2	-94.2
Oper	-10.5	-7.7	-11.1
McRad	-7.2	-4.5	-7.9
SNET ocn	-2.1	-0.9	-7.9
Oper	-8.1	3.6	-17.3
McRad	2.8	14.0	-6.8

Table 2 Results from 13-month simulations at $T_159 L91$. Radiative fluxes at TOA are compared to CERES measurements, total cloud cover (TCC) to ISCCP D2 data, total column water vapour (TCWV) and liquid water (TCLW) to SSM/I data. TP is the total precipitation compared to GPCP or SSM/I data. The surface fluxes are compared to the Da Silva climatology. Numbers in brackets are standard deviation.

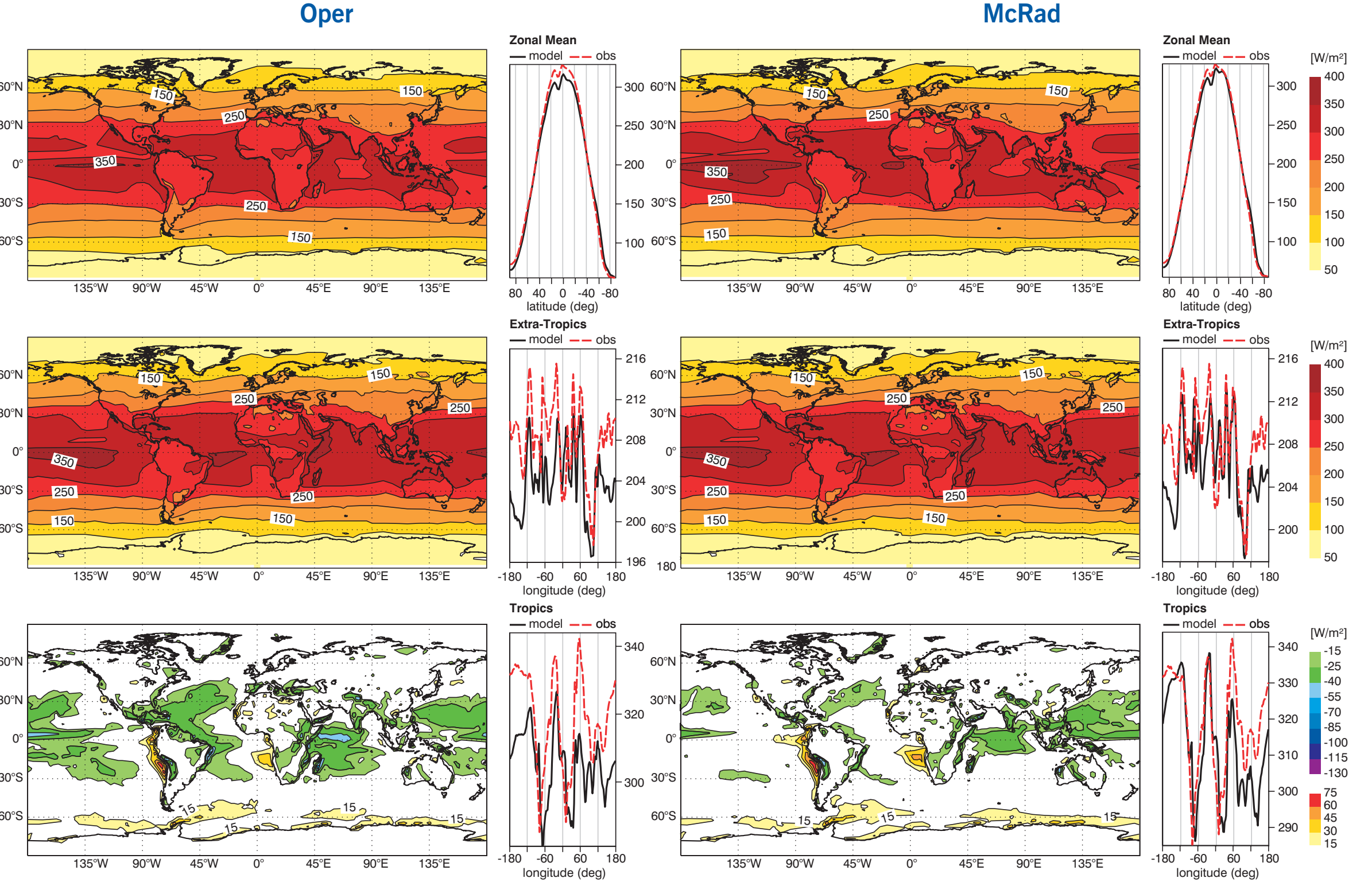


Figure 3 The longwave cloud forcing ($W m^{-2}$). Top figures are the ECMWF model simulations (left: operational, right: McRad), middle ones are the CERES observations, bottom ones are the differences between simulations and observations.

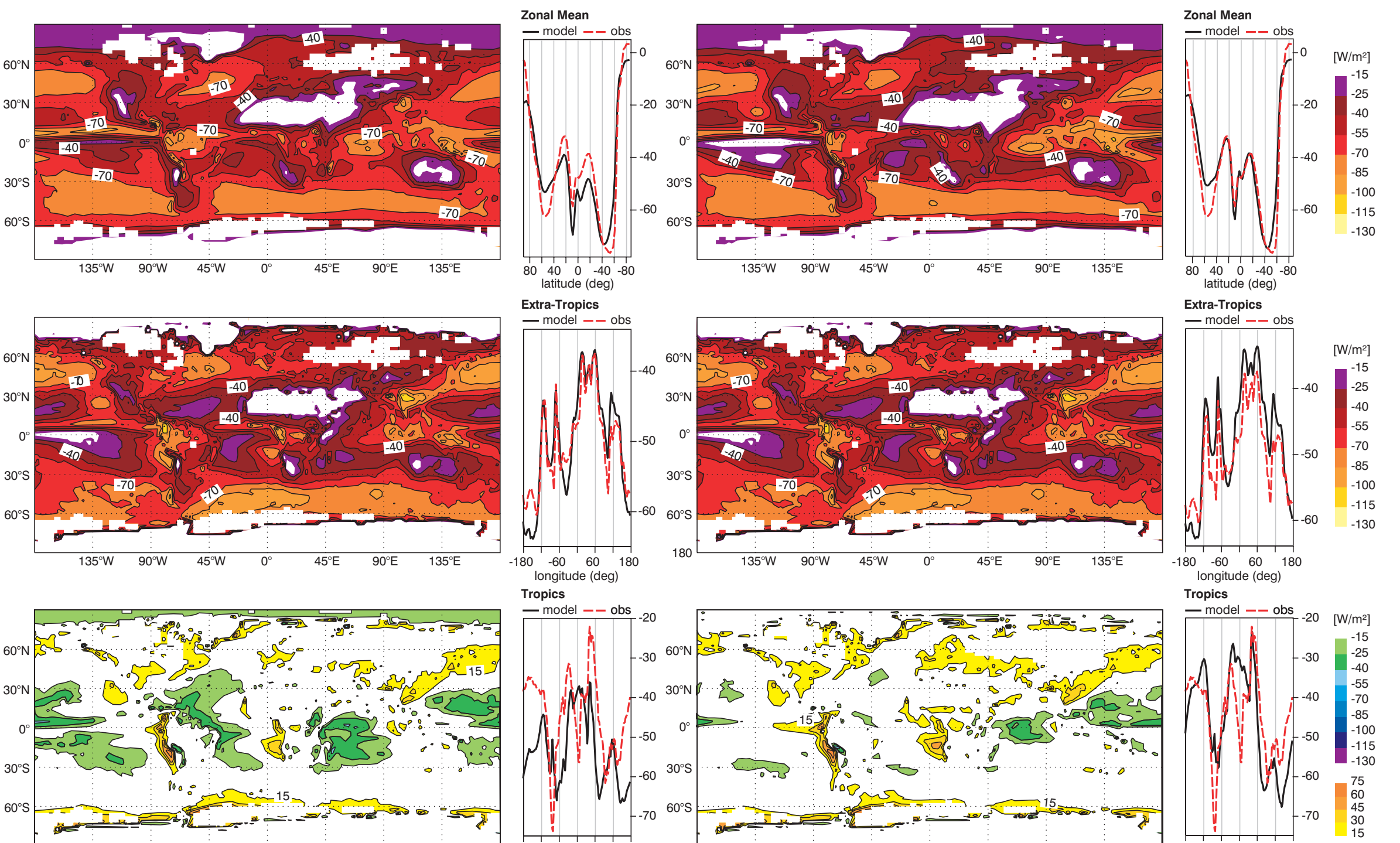


Figure 4 The shortwave cloud forcing ($W m^{-2}$). Top figures are the ECMWF model simulations (left: operational, right: McRad), middle ones are the CERES observations, bottom ones are the differences between simulations and observations.

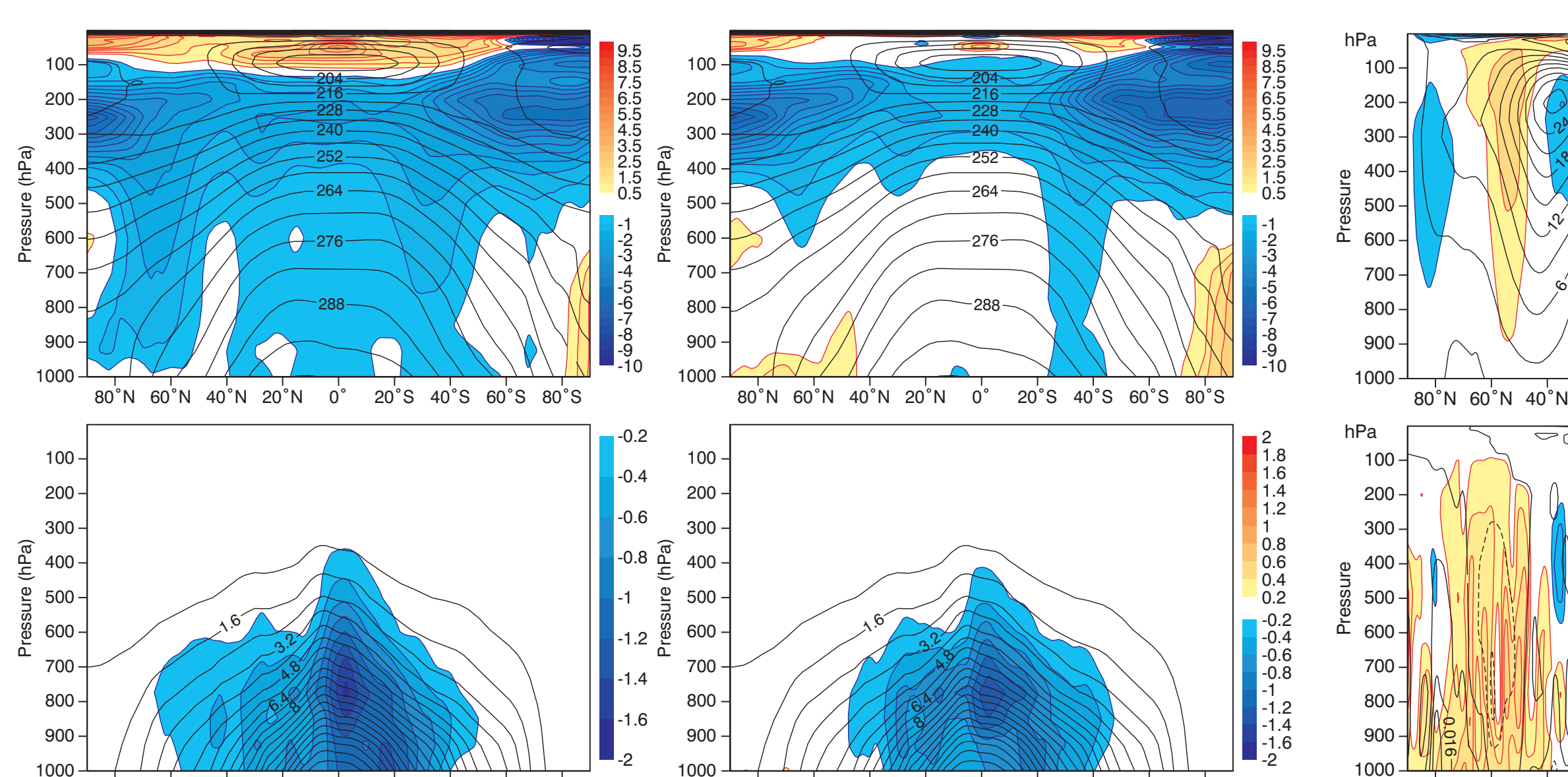


Figure 5 The difference with ERA40 analysis for temperature (top panels, in K) and humidity (bottom panels, in $kg kg^{-1}$). Left column is for the operational model; right one for the model with McRad.

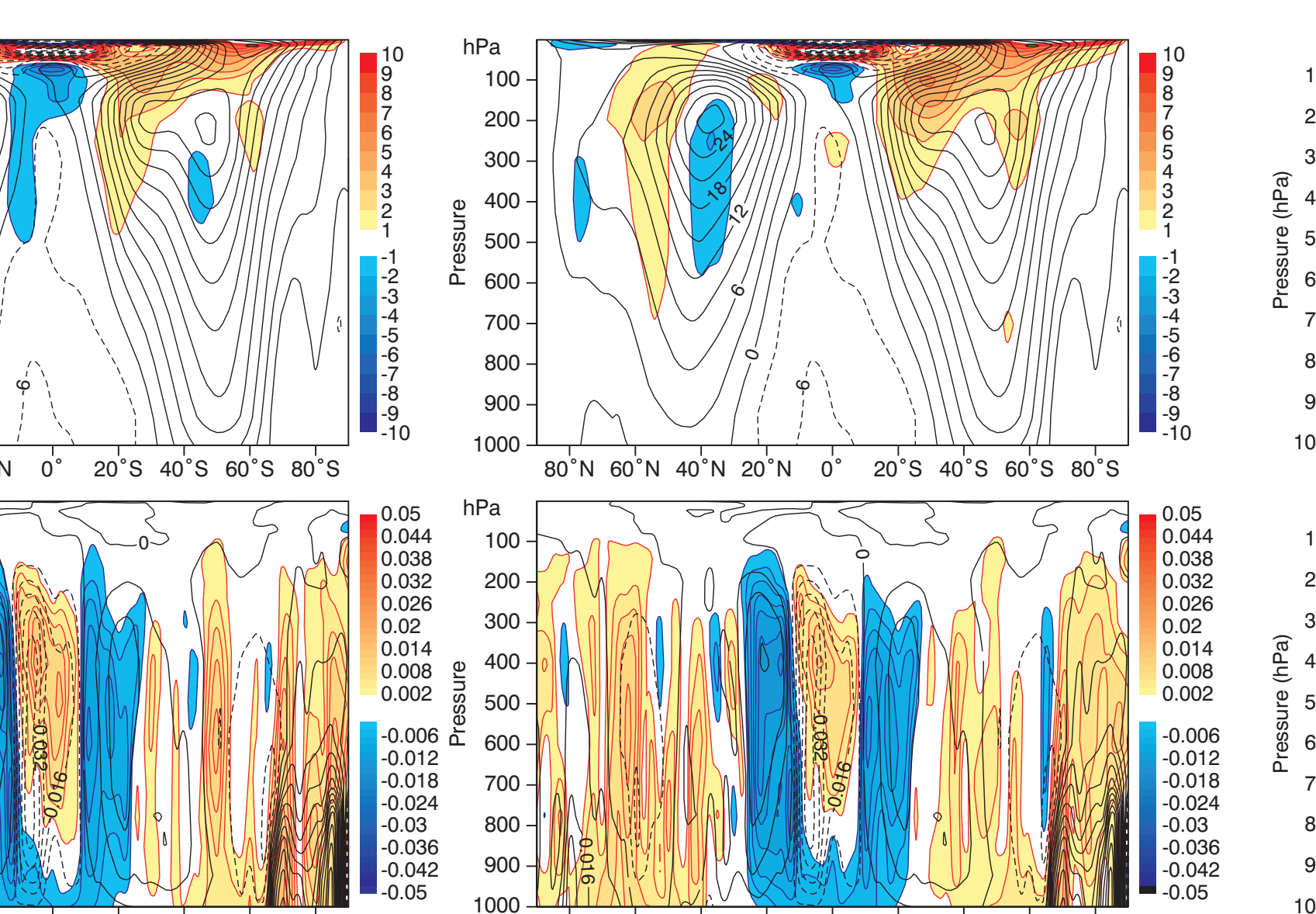


Figure 6 The difference with ERA40 analysis for zonal wind (top panels, in $m s^{-1}$) and vertical velocity (bottom panels, in $Pa s^{-1}$). Left column is for the operational model; right one for the model with McRad.

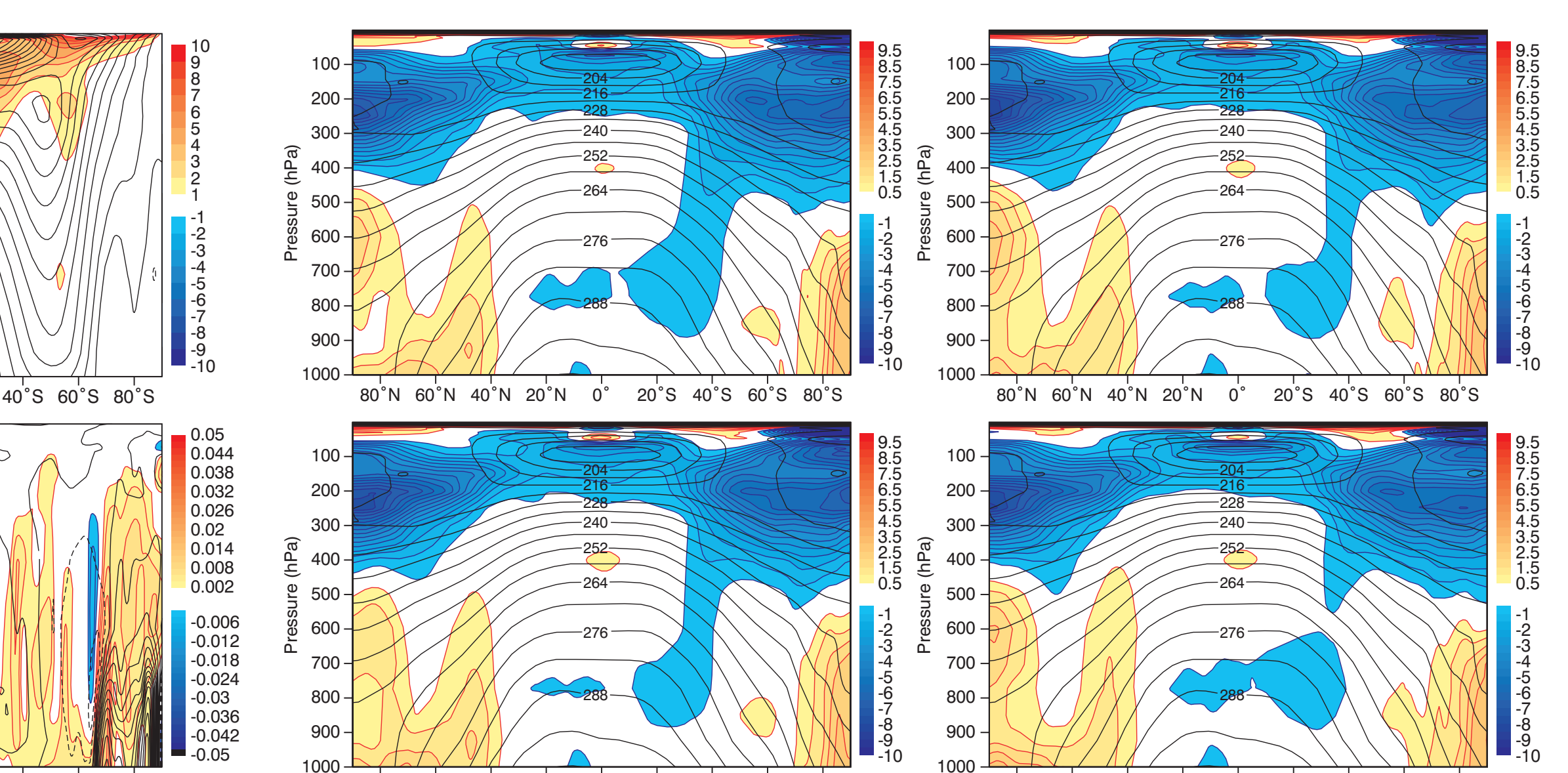


Figure 7 The difference with ERA40 analysis for temperature (top panels, in K). Top left is the McRad model with generalized overlap of cloud layers with a decorrelation length for cloud cover DLCC = 2 km and a decorrelation length for cloud water DLCW = 1 km, top right with DLCC = 4 km and DLCW = 2 km, bottom left with DLCC = 5 km and DLCW = 1 km. Bottom right is the McRad model with maximum-random overlap of homogeneous clouds.

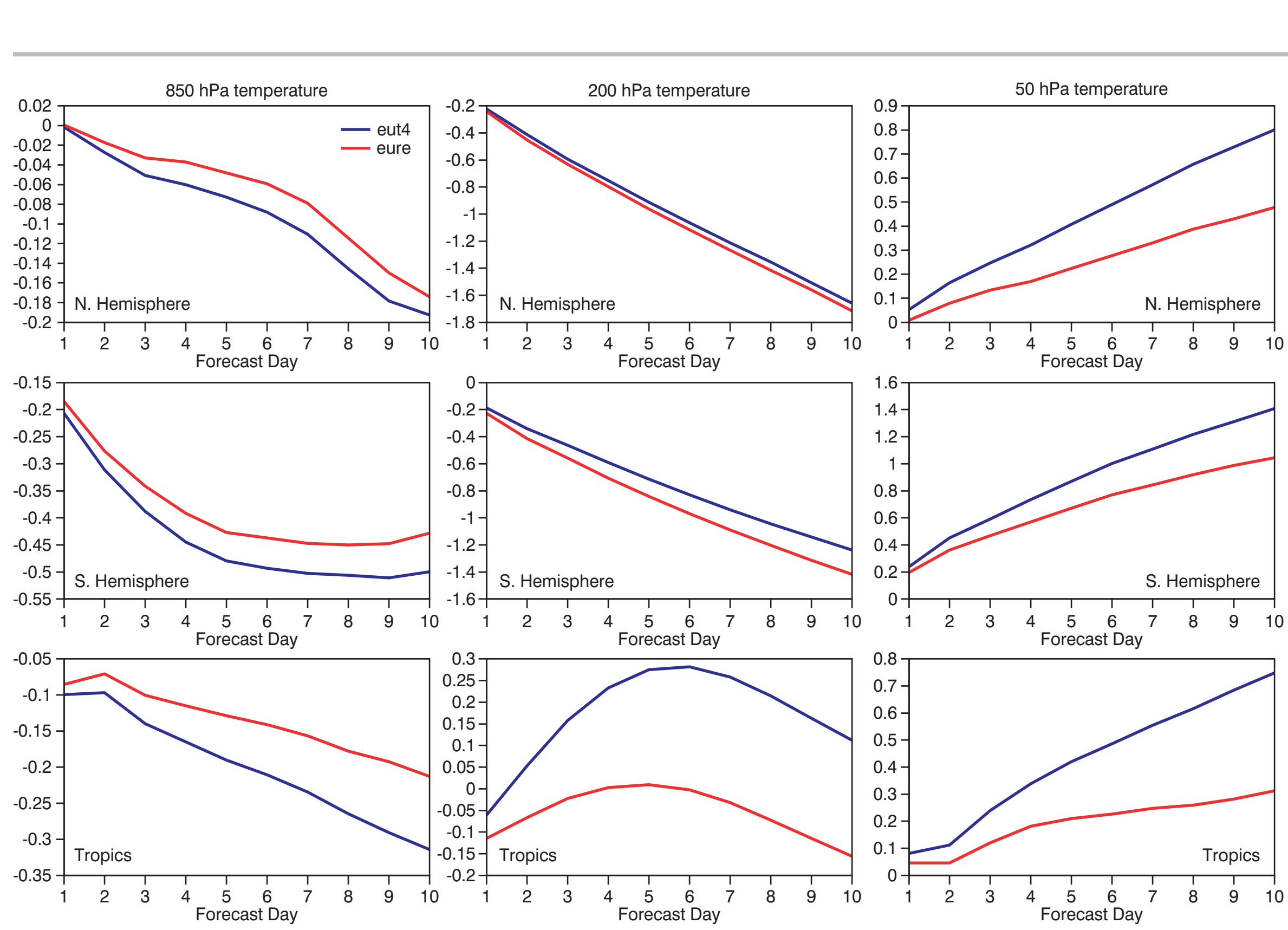


Figure 7 The mean error of the temperature for a set of 108 10-day forecasts at $T_319 L91$, started every 24 hours from 20060531 12 UTC. Top to bottom, Northern Hemisphere, Southern Hemisphere, Tropics $20^{\circ}N$ – $20^{\circ}S$. Reference in blue, McRad in red. Left column is for 850 hPa, middle for 200 hPa, right for 50 hPa.

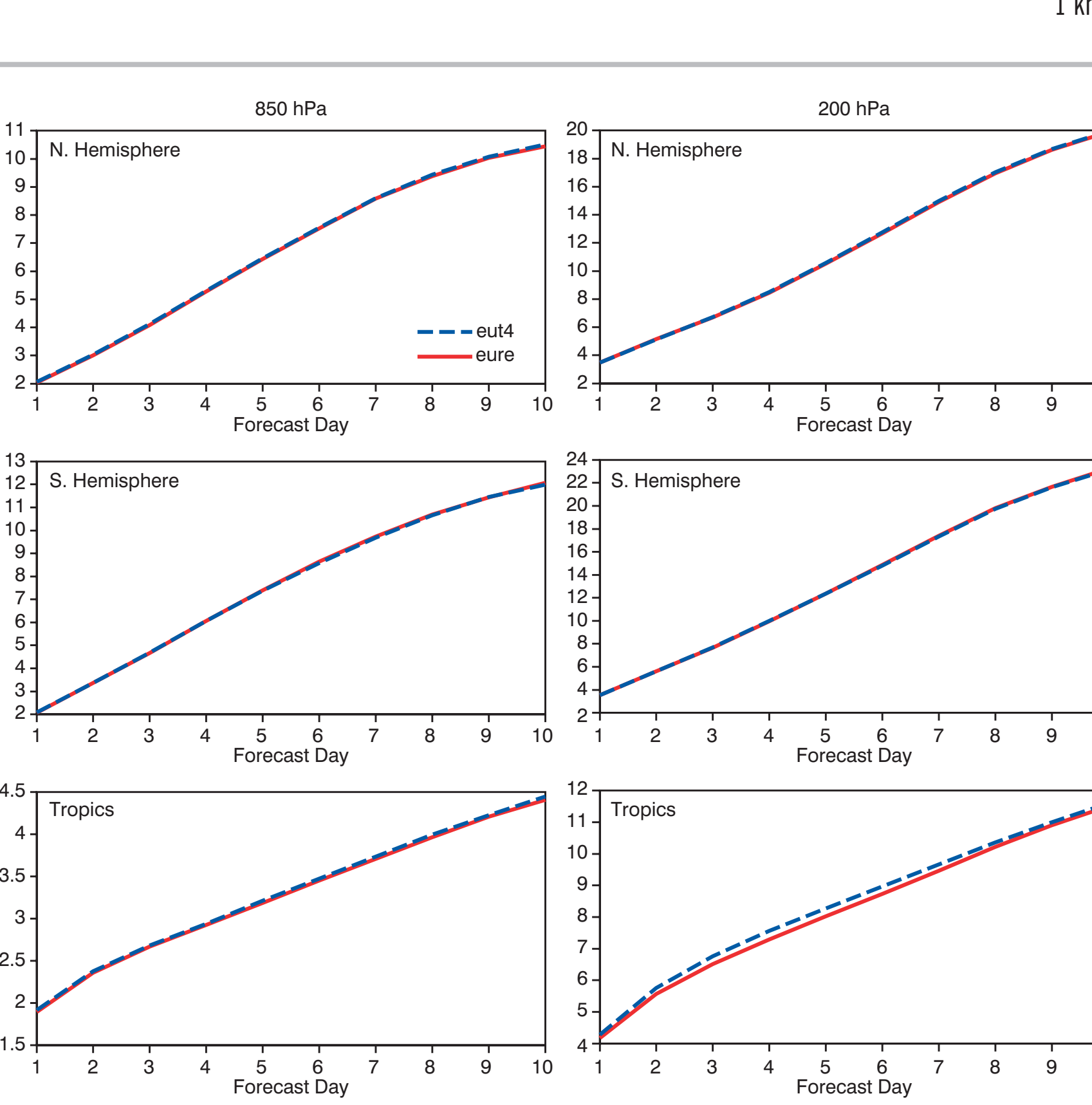


Table 3 Results from 13-month simulations at $T_{159} L91$ with different cloud configurations. G21 is the McRad model with generalized overlap of cloud layers with a decorrelation length for cloud cover DLCC = 2 km and a decorrelation length for cloud water DLCW = 1 km, G42 is with DLCC = 4 km and DLCW = 2 km, G51 is with DLCC = 5 km and DLCW = 1 km. MR is the McRad model with maximum-random overlap of homogeneous clouds. All quantities are annual means. Radiative fluxes at TOA are compared to CERES measurements, total cloud cover (TCC) to ISCCP D2 data, total column water vapour (TCWV) and liquid water (TCLW) to SSM/I data. TP is the total precipitation compared to GPCP or SSM/I data. The surface fluxes are compared to the Da Silva climatology.

Acknowledgments

Drs E. Mlawer, M. Iacono, J. Delamere, and A. Clough (AER, Inc.) provided both the original RRTM longwave and shortwave radiation codes, that were adapted to the ECMWF model and modified to include the McICA approximation to deal with cloudiness. Drs H. Barker and R. Pincus convinced the author to initiate this work and maintained the pressure till McICA was properly tested in the ECMWF IFS. Dr P. Raisanen wrote the cloud generator, and Dr J. Cole answered a number of queries on the cloud generator. At ECMWF, Drs D. Salmon and J. Hague helped in the debugging and optimization of the code.

References

- Barker, H.W., R. Pincus, and J.-J. Morcrette, 2003b: The Monte-Carlo Independent Column Approximation: Application within large-scale models. *Proceedings GCSS/ARM Workshop on the Representation of Cloud Systems in Large-Scale Models*, May 2002, Kananaskis, AB, Canada, 10 pp.
- Mlawer, E.J., and S.A. Clough, 1997: Shortwave and longwave enhancements in the Rapid Radiative Transfer Model. In *Proceedings of the 7th Atmospheric Radiation Measurement (ARM) Science Team Meeting*, U.S. Department of Energy, CONF-9603149. <http://www.arm.gov/publications/proceedings/conf07title.htm>.
- Mlawer, E.J., S.J. Taubman, P.D. Brown, M.J. Iacono, and S.A. Clough, 1997: Radiative transfer for inhomogeneous atmospheres: RRTM, a validated correlated-k model for the longwave. *J. Geophys. Res.*, 102, 16,663–16,682.
- Morcrette, J.-J., 2007: Impact of a New Radiation Package in the ECMWF Integrated Forecast System. *Proceedings ECMWF Cloud Workshop*, 13–15 November 2006.
- Pincus, R., H.W. Barker, and J.-J. Morcrette, 2003: A fast, flexible, approximate technique for computing radiative transfer in inhomogeneous clouds. *J. Geophys. Res.*, 108, 4376, doi:10.1029/2002JD003322.